Transient dynamical analysis of a dual-rotor system excited by a sudden loss of mass of blade

Jin Huang[1], Yuefang Wang[2]

[1]Dalian University of Technology, Dalian116024, Liaoning, China
[2]Dalian University of Technology, Dalian116024, Liaoning, China

*Corresponding author: yfwang@dlut.edu.cn

Abstract

The transient dynamics of a high speed rotor assembly of a gas turbine is presented in this paper demonstrates that the blade loss will significantly influence to the rotor. To theoretically investigate the motion stability of the system, a reduced rigid Jeffcott rotor model with symmetrical short bearings is presented. The equations of motion are derived considering the nonlinear lubricant forces of bearings. The transient response of the rotor is numerically obtained through the Runge-Kutta scheme with adaptable step-sizes. It is shown that the equilibrium of the rotor is disturbed due to the sudden loss of mass. However, the stability of motion can be restored. Bifurcation diagrams are constructed to investigate the responses of the rotor at various the rotation speeds at a specific eccentricity. The largest Lyapunov exponent (LLE) diagram has been presented to indicate when the system evolves into chaos.

Keywords: blade loss; Jeffcott rotor; largest Lyapunov exponent

Introduction

Rotors of gas turbines are required to operate at supercritical speeds. Structurally, most modern gas turbines are in form of twin spools and are composed of an axial compressor and a power turbine that rotates with different speeds and is supported by rolling bearings as well as intermediate bearings. Due to the complexity in both structure and loading of the rotor, it is very hard to obtain analytical solution of the rotor assembly. The transient response of the rotor is influenced by many loading effects. The most dominant of them is the loss of blades of the impellers. In practical operations of the gas turbine, there is a possibility that one blade of impellers breaks off which causes a sudden loss of mass. Consequently, an impulsive imbalance of mass is generated in the transverse direction of the rotor shafts. This unbalance leads to unexpected large motions. Hence, a detailed blade loss transient response of the rotor system should be conducted.

Since it is time consuming to obtain the dynamical characteristics of the rotor by performing various transient response analyses, the rotor is reduced to a 2-DOF Jeffcott system (Jing, 2004) in this study to obtain the essential dynamical properties of the system. The transient nonlinear lubricant force is necessary for obtaining transient response of the rotor system. The available approximate methods for the slide bearing can be classified as follows. The direct methods, such as difference or finite element method, tackle with the Reynolds equation directly to get the pressure distribution, and the transient oil film force can be obtained by integrating the acquired pressure of oil film. Based on variational method, the variational model (Xia and Qiao, 2009) has relatively high accuracy, but lots of variational iterations are needed to get the proper boundaries which will great reduce the efficiency. The approximate analytic methods claims simple and high accuracy for bearings with small length-to-diameter ratio and the Capone model (Adiletta, 1996) has been widely accepted which will also be implemented in this study.

In this paper, the dynamics of a dual rotor system is presented with specified unbalanced mass distribution on the rotor impellers. To simulate the situation of sudden loss of mass of blade, a concentrated mass imbalance is created and placed on the third impeller of the compressor. The Runge-Kutta method with adaptable step size is implemented to perform the numerical integration of the governing equation. It is demonstrated that the motion of the rotor system will be asymptotic stable when it is disturbed from the equilibrium position. With the journal center staying at the balanced position, a sudden step or ramp unbalance load is applied on the rotor, respectively, and the motions of the system are investigated subsequently. The results show that in both cases a periodic orbit corresponding to a limit cycle will be generated with a slight difference between them. Bifurcation diagrams are generated based on the Poincaré section to present the responses of the rotor with varying rotational speeds. The results indicate that the system will enter the state of chaos through a complicate route when the rotation speed increases high enough. The largest Lyapunov exponent diagram has been presented to indicate when the motion of the system evolves into chaos.

Transient response of a twin spool rotor

The twin-spool rotor of the gas turbine is shown in Fig.1(a), which was first studied by (Guangyoung and Palazzolo, 2008). The rotor is supported by six rolling element bearings numbered as #0 through #5 and composed of two parts, inner power turbine and outer compressor. Two intermediate bearings, i.e. IDB 1 and IDB 2 are used to connect the power turbine with the compressor. The parameters of stiffness and damping of the bearings are listed in Table 1.Fig.1(b) shows the finite element model created with software SAMCEF/Rotor using two dimensional axisymmetric elements. The total numbers of element and node are 477 and 269, respectively. Three concentrated masses are placed on points 1, 2 and 3 to represent the mass unbalances on the first three blades of the compressor. The place where the blade loss occurs coincides with the third mass unbalance. Their values are assigned in Table 2.

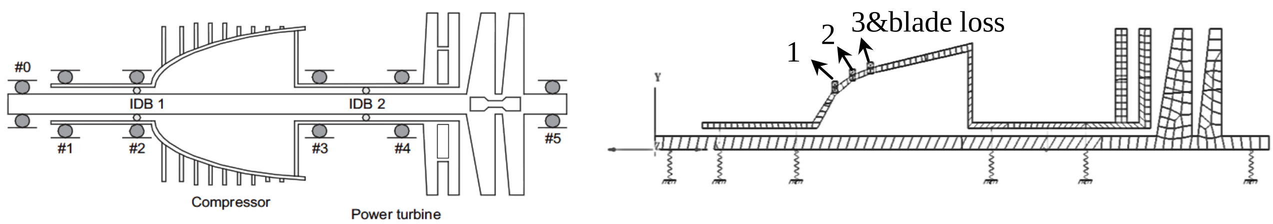

(a) (b)

Figure 1 (a) Scheme of a twin spool rotor; (b) FEM model of the rotor.

The operating speeds of the power turbine and the compressor are 13,000rpm and 20,000 rpm, respectively. To get the transient response, a set of unbalanced masses are assigned to the impellers which are shown in Table 1 and their locations can be found as numbered points 1, 2, and 3 in Fig.1(b).

Table 1 Stiffness and damping coefficients of bearings

Bearing No.	Stiffness (10^8 N/m)	Damping(10^3 Ns/m)
#0~#5	1.75	1.75
IDB1	0.875	3.502
IDB2	0.875	3.502

Table 2 Unbalanced masses on impellers. "B.L." means blade loss.

Unbalance No.	Mass(kg)	Eccentricity (mm)	Phase (degree)
1	1.41	0.635	45
2	1.21	0.635	45
3	1.11	0.635	45
B.L.	1.11	3.175	45

Fig.2(a) shows the operation speed profiles of start-up of the power turbine and compressor for creating the load of transient analysis. The speed profile is approximated by a series of straight lines for simplicity. Herein, it is assumed that the normal operation speed of the rotor remains unchanged after the occurring of blade loss. The blade loss will result in a time-varying redistribution of the unbalances of the rotor system. An impulsive unbalance of mass is imposed on the rotor to simulate this process whose continuous effect to the system is achieved through the change of rotation speed with a different speed profile from the one of rotor.

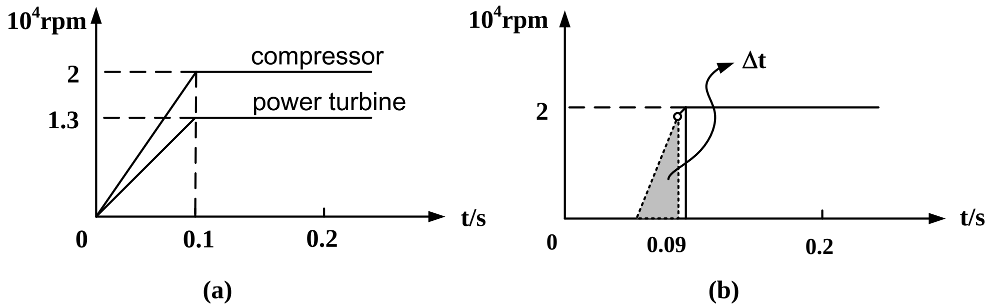

Figure 2: (a) Profile of engine start-up and operation; (b) Profile of blade loss during start-up. Δt represents the duration of blade loss

The transient response with Δt=0.01s compared to the case of without blade loss case is shown in Fig.3. The maximum amplitude of the transient response of the system occurs at 0.97s. The motion will decay to a steady state after a transient fluctuation. One can observe that the blade loss has generated a large amplitude transient response; hence it is of great importance to perform the blade loss response analyses for the rotor system.

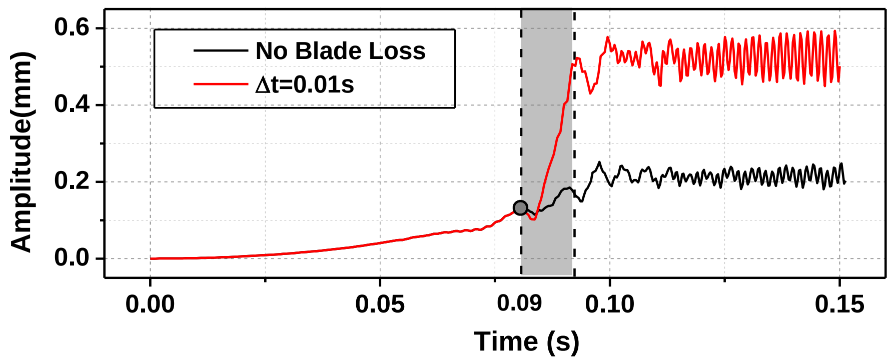

Figure 3 Transient responses at Δt=0.01s. The shadowy area represent the duration of the blade loss.

Transient response of a Jeffcott rotor

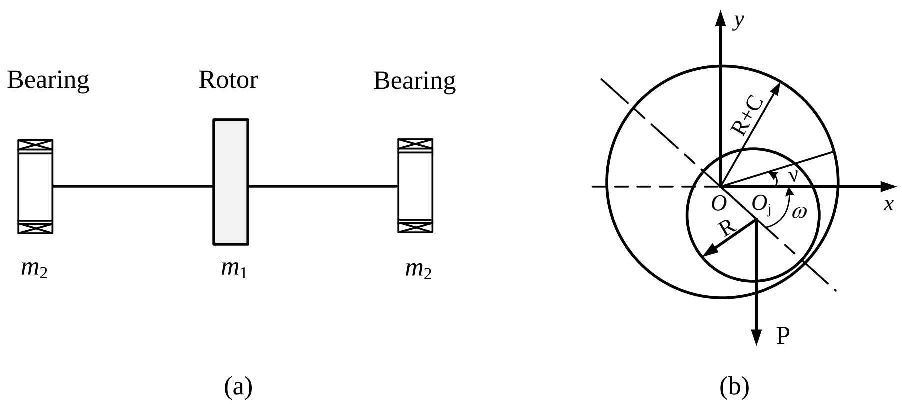

Figure 4: (a) Rotor system with short journal bearings; (b) Cross-section of the journal.

Generally, it is time consuming to obtain the dynamical characteristics of the rotor by performing various transient response analyses; the rotor is reduced to a 2-DOF Jeffcott system in this study. The mass of the rotor is 120kg, the first order critical speed ω_1 =152Hz. Hence, the equivalent stiffness of the rotor is $k_e = m\omega_1^2$ =1.1×10^8 N/m. The slide oil film bearings are included in the simplified model to investigate the transient dynamics of the system with nonlinear bearing forces. Fig.4(a) presents the rotor supported by symmetric bearings which is subjected to both static unbalance and external load. The equations of the motion of the journal center O_j are

$$\begin{cases} m_1\ddot{X}_1 = -k_e(X_1 - X_2) + F_x, \quad m_1\ddot{Y}_1 = -k_e(Y_1 - Y_2) + F_y - P_1 \\ m_2\ddot{X}_2 = -2k_e(X_2 - X_1) + m_2 e\omega^2\cos(\omega t), \quad m_2\ddot{Y}_2 = -2k_e(Y_2 - Y_1) + m_2 e\omega^2\sin(\omega t) - P_2 \end{cases} \tag{1}$$

where P_1 and P_2 are gravity loads, F_x and F_y are supporting forces to the rotor considering both the reaction force from the bending shaft and the oil-film forces from the bearings. The dimensionless form Eq.(3) of Eq. (1) can be obtained with the following substitutions:

$$\begin{cases} x = \dfrac{X}{C}, \quad y = \dfrac{Y}{C}, \quad \tau = \omega t, \quad \dot{x} = \dfrac{\dot{X}}{C\omega}, \quad \dot{y} = \dfrac{\dot{Y}}{C\omega}, \quad \ddot{x} = \dfrac{\ddot{X}}{C\omega^2}, \quad \ddot{y} = \dfrac{\ddot{Y}}{C\omega^2}, \\ \rho = \dfrac{e}{C}, \quad f_x = \dfrac{F_x}{\delta P}, \quad f_y = \dfrac{F_y}{\delta P}, \quad G = \dfrac{g}{\omega^2 C}, \quad m_{22} = \dfrac{m_2\omega^2 C}{\delta}, \ k = \dfrac{k_e}{\omega^2} \end{cases} \tag{2}$$

In this situation, f_x and f_y are dimensionless Journal supporting forces. The analytical form of the nonlinear journal force of the short bearing model proposed by Capone (Adiletta, 1996) is adopted in this study.

$$\begin{cases} \ddot{x}_1 = -\dfrac{2k}{m_1}(x_1 - x_2) + \rho\cos\tau, \ \ddot{y}_1 = -\dfrac{2k}{m_1}(y_1 - y_2) + \rho\sin\tau - G \\ \ddot{x}_2 = -\dfrac{k}{m_2}(x_2 - x_1) + \dfrac{1}{m_{22}} f_x, \ \ddot{y}_2 = -\dfrac{k}{m_2}(y_2 - y_1) + \dfrac{1}{m_{22}} f_y - G \end{cases} \tag{3}$$

The Runge-Kutta method with adaptable step size is implemented to perform the numerical integration of the governing equation.

The parameters listed in Table 3 are used to compute the transient responses of the rotor impulsively loaded by a step and a ramp mass unbalance load, respectively. The profiles of loads are given by Fig.5. Similar to the previous 2D case, the blade loss process is simulated by the continuous redistribution of the unbalance mass ρ with time , where the dimensional time is 10/π≈ 3.2s.

For the case ρ=0, where the system only bear the gravity load under a specific speed, the orbit is illustrated in Fig.6(a). It is observed that the equilibrium positions of m_1 and m_2 are (0.4256, -0.3702) and (0.4256, -0.3824), from which we have $x_1 = x_2$. In light of Eq. (3), the *x*-acceleration is equal to zero and f_x should be and indeed is zero which ensures that m_2 is in a balanced state. The fact that y_1 and y_2 are not equal is intended to generate lubricant forces to balance the gravity loads.

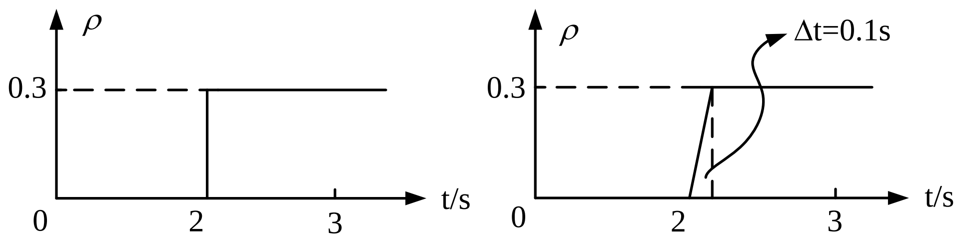

(a) (b)

Figure 5 (a) Profile of step load, (b) Profile of ramp load

Table 3 Parameters of the rotor under gravity loads at a specific rotation speed

Item	Value
Rotor mass(kg)	114.4
Diameter(m)	0.08
Length(m)	0.03
Oil film gap(m)	0.0002
Kinetic oil viscosity(Pa·s)	0.0115
Rotation angular speed(rad/s)	100π
Computing time (dimensionless)	1000
Eccentricity ρ of the load case	0.1
Stiffness of half shaft(N/m)	1.1×10^{8}
Initial coordinate (x_1, y_1, x_2, y_2)(dimensionless)	0.1, 0.1 ,0.15, 0.15
Initial velocity ($\dot{x}_1, \dot{y}_1, \dot{x}_2, \dot{y}_2$)(dimensionless)	-0.1, 0.1 ,-0.1 ,0.1

From Fig.6(a) it is observed that the two orbits of m_1 and m_2 are almost overlap, hence in the following study only the orbit of m_1 is selected as the research object. Fig.6(b) and (c) show the trajectories of the journal center when a sudden unbalance step or ramp load is applied after the journal converges to its equilibrium. The two load profiles are given by Fig.5(a). The unbalance force will push the journal away from the equilibrium center and eventually drives it to an orbit of stable limit cycle. Naturally, the ramp load case needs a longer time to progress to the limit cycle. From Fig.7, it is observed that the maximum transient amplitude of the step load be a little larger than the one of the ramp load and the rotor in both cases will evolve into an identical orbit in the end.

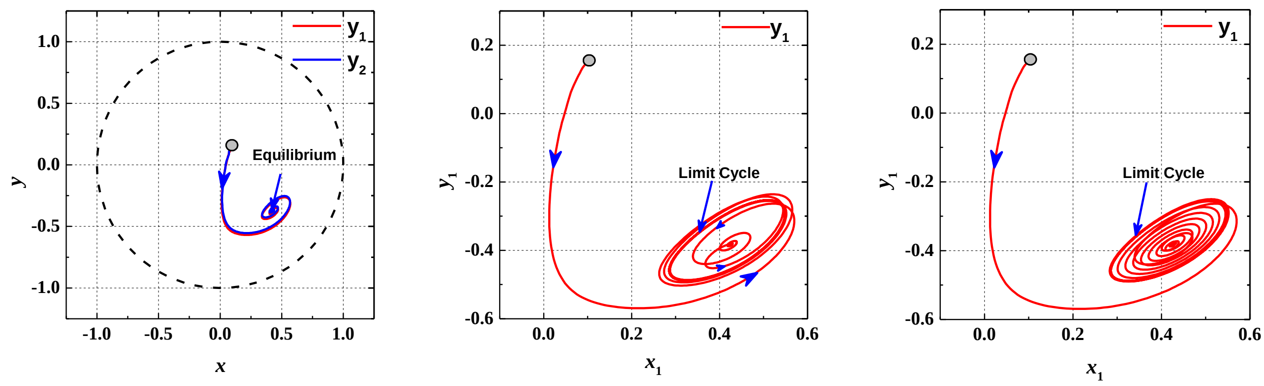

(a) (b) (c)

Figure 6 Results under different loads: (a) Orbit under gravity load; (b) Orbit under step load; (c) Orbit under ramp load.

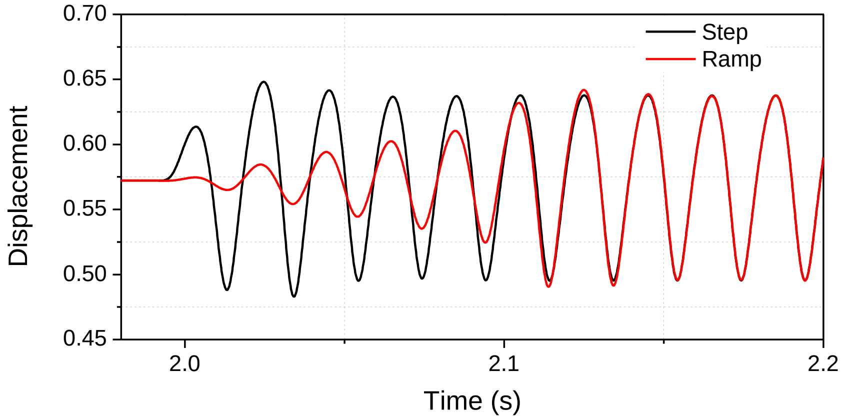

Figure 7 Comparison of the transient response of the step load and ramp load

At ρ=0.1, the LLE diagram (Fig.8(a)) is generated with the Benettin method (Benettin, G. and L. Galgani, 1980). The rotor is in chaotic state at the corresponding speed when the LLE is large than zero. It can be observed that the LLE diagram coincides with the two bifurcation diagrams. Two bifurcation diagrams shown in Fig.8(b) and (c) are designated to investigate the responses of the rotor with varying rotation speeds. The results show that the rotor undergoes small amplitude period motions orbiting around the equilibrium when the speeds less than 540 rad/s. After a short period of quasi-periodic evolution in the interval (540,556) rad/s, the rotor goes into a double-period orbit when the speed reaches 556 rad/s. After the speed rises up to 630rad/s, the rotor suddenly enters chaotic state at 680rad/s. Then, the rotor undergoes a short period of double period again before it evolves into another chaotic state at 768rad/s. On the whole, it is observed that the route of the state of the system from period motion to chaos is very complicated.

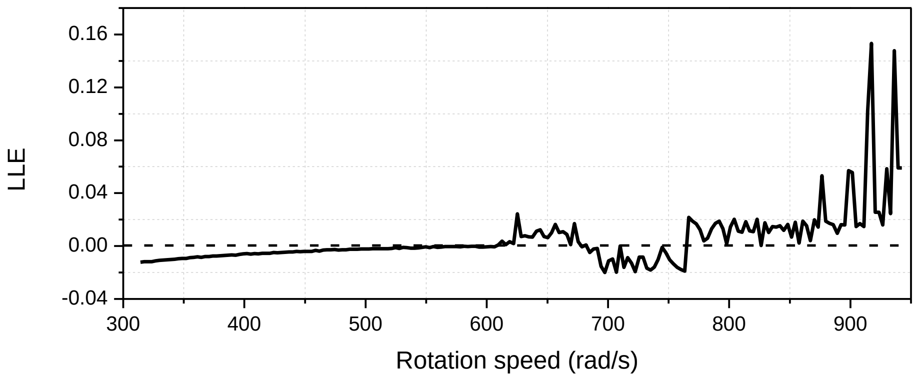

(a)

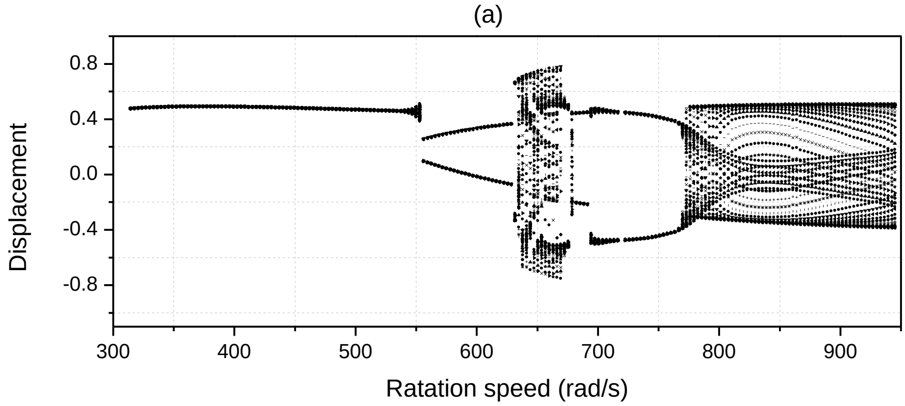

(b)

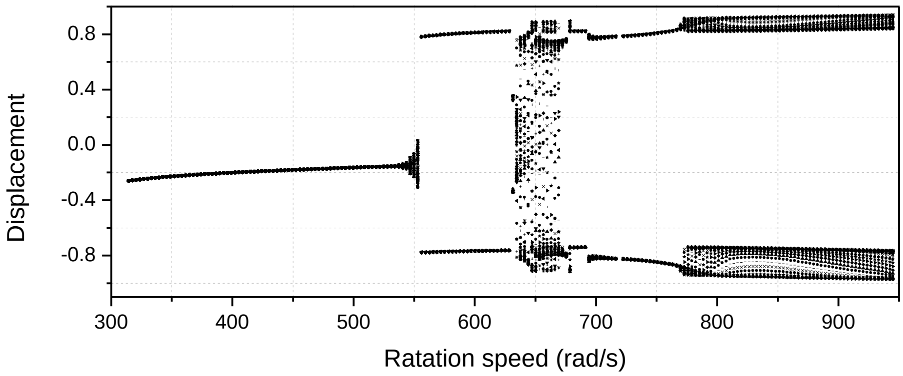

(c)

Figure 8 Results of variation rotation speeds, (a) Largest Lyapunov exponent diagram; (b) bifurcation diagram of x_1; (c) bifurcation diagram of y_1.

Conclusions

In this paper, two transient analyses of both a real engine rotor and a theoretical Jeffcott rotor have been conducted. A transient response analysis is conducted for start-up of the twin spool rotor shows that the blade loss will significantly influence the maximum transient response of the rotor.

Next, considering it is time consuming to perform lots of transient analysis with the 2D FEM model to get the dynamical properties of the rotor, a reduced Jeffcott rotor model supported by symmetrical slide bearings under step and ramp sudden unbalance loads has been investigated. The results show that the system will recover to a stable motion after undergoing unbalance impacts while the maximum amplitude resulting from the step load is larger than the one from ramp load. At a specific eccentricity, Poincaré sections have been constructed to investigate the responses of the rotor when the rotation speed changes. The bifurcation diagrams of displacements show that the route of the system evolves into chaos are complicated. The largest Lyapunov exponent diagram shows a good correspondence of the bifurcation diagram in indicating when the rotor evolves into chaos.

Acknowledgments

The authors are grateful for the support from the State Key Development Program for Basic Research of China (Projects 2009CB724300 and 2011CB706504). The advice from Mr. Feng Guoquan in preparation of this paper is appreciated.

References

Adiletta G., Guido A. R., Rossi C. (1996), Chaotic motions of a rigid rotor in short journal bearings. *Nonlinear Dynamics*, 10, pp.251-26.

Benettin, G. and Galgani L. et al. (1980), Lyapunov Exponents for smooth dynamical systems and for Hamiltonian systems; A method for computing all of them. Part 2: Numerical application. *Meccanica*, 15, pp. 21-30.

Guangyoung, S. and A. Palazzolo, et al. (2008), Long duration blade loss simulations including thermal growths for dual-rotor gas turbine engine. *Journal of Sound and Vibration*, 316, pp. 147-163.

Jing J. P. and Guan M., et al. (2004), On the non-linear dynamic behavior of a rotor–bearing system. *Journal of Sound And Vibration*, 274, pp. 1031-1044.

Xia, Z. P. and Qiao G. et al. (2009). Nonlinear modeling and dynamic analysis of the rotor-bearing system. *Nonlinear Dynamics*, 57, pp. 559-577.